DBEM crack propagation for nonlinear fracture problems

R. Citarella, V. Giannella, M. Lepore
Dept. of Industrial Engineering, University of Salerno, via G. Paolo II, 132, Fisciano (SA), Italy
rcitarella@unisa.it

ABSTRACT. A three-dimensional crack propagation simulation is performed by the Dual Boundary Element Method (DBEM). The Stress Intensity Factors (SIFs) along the front of a semi elliptical crack, initiated from the external surface of a hollow axle, are calculated for bending and press fit loading separately and for a combination of them. In correspondence of the latter loading condition, a crack propagation is also simulated, with the crack growth rates calculated using the NASGRO3 formula, calibrated for the material under analysis (steel ASTM A469). The J-integral and COD approaches are selected for SIFs calculation in DBEM environment, where the crack path is assessed by the minimum strain energy density criterion (MSED). In correspondence of the initial crack scenario, SIFs along the crack front are also calculated by the Finite Element (FE) code ZENCRACK, using COD, in order to provide, by a cross comparison with DBEM, an assessment on the level of accuracy obtained. Due to the symmetry of the bending problem a pure mode I crack propagation is realised with no kinking of the propagating crack whereas for press fit loading the crack propagation becomes mixed mode. The crack growth analysis is nonlinear because of normal gap elements used to model the press fit condition with added friction, and is developed in an iterative-incremental procedure.
From the analysis of the SIFs results related to the initial cracked configuration, it is possible to assess the impact of the press fit condition when superimposed to the bending load case.

KEYWORDS. DBEM; Crack Propagation; Nonlinear Fracture Mechanics.

INTRODUCTION

The crack growth analysis of flaws is one of the most important parts for structural integrity prediction of metallic components in the presence of initial and accumulated in-service damages. The problem of residual fatigue life prediction with non-linear loading conditions in structural elements is complex and analytical solutions are generally not available.
In the present study, the Dual Boundary Element Method (DBEM) [1], as implemented in the commercial software BEASY [2], is used to simulate the stress scenario on a hollow cylinder, loaded with non-linear boundary conditions.
The Stress Intensity Factors (SIFs) are calculated by both the COD (Crack Opening Displacement) [3-5] and the J-integral [6-11] approaches for different load cases: pure bending, press-fit (involving nonlinear contact conditions at the interface between hub and axle) [12] and a combination of them, to understand the impact on the crack of each load case (bending and press fit). Then, the growth of the semi-elliptical crack, initiated from the axle surface, is simulated considering the simultaneous application of bending and press-fit and using the Minimum Strain Energy Density (MSED) criterion for crack path assessment [13]. When considering the crack propagation the SIFs from J-integral approach are adopted.

From the analysis of the SIF results related to the initial cracked configuration (for such scenario also SIF results obtained by the FEM code ZenCrack have been added for cross comparison), it is possible to assess the impact of the press fit condition when superimposed to the bending load case. Due to the symmetry of the problem a nearly pure mode I crack propagation is realised (K_{II} and K_{III} turn out to be negligible) with no kinking of the propagating crack. The crack growth analysis is nonlinear because of normal gap elements used to model the press fit condition with added friction, and is developed in an iterative-incremental procedure.

PROBLEM DESCRIPTION AND DBEM MODEL

Introduction

The case study, designed by Sander et Al. [14], represents a four point bending hollow axle in a symmetric configuration (Figs. 1, 2), so that just half axle needs to be modeled in the DBEM environment.
Three different load cases have been considered:

- bending load case;
- press fit load case;
- combined load case with simultaneous allowance for bending and press fit.

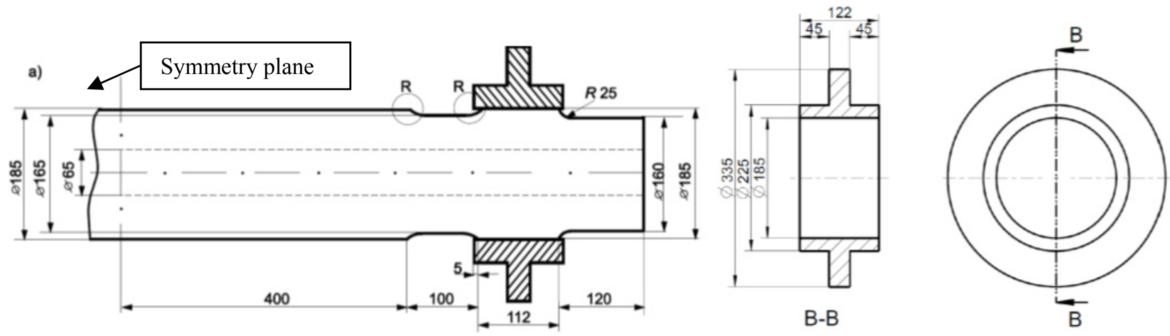

Figure 1: Drawing of the hollow axle and hub, with highlight of the symmetry plane.

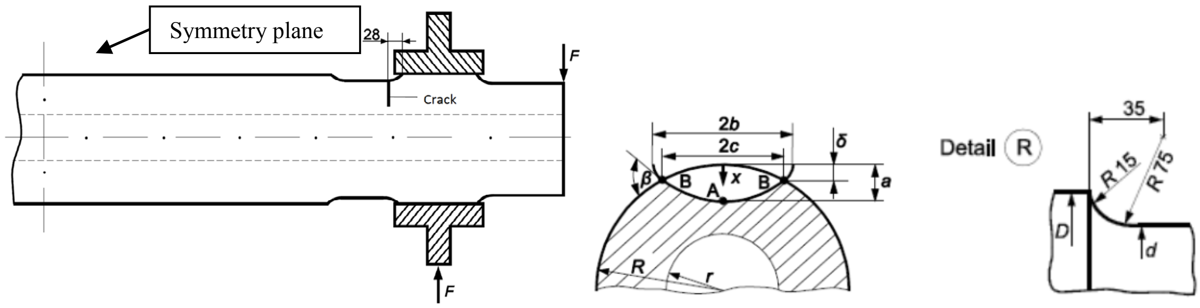

Figure 2: Drawing of the cracked hollow axle with detail view of crack and fillet double radius.

Uncracked DBEM model

The DBEM model is made up of two different zones, one for the axle and the other for the hub; the mesh is based on quadrilateral or triangular elements with quadratic shape functions and is not needed on the symmetry plane (Fig. 3).
The bending load is obtained by applying a uniform traction distribution on one axle side, whose resultant force is equal to 200 kN, and a point force, equal to 200 kN, in the hub; springs of negligible stiffness are added (on the internal diameter, close to the symmetry plane) in X, Y, Z directions to apply the rigid body constraints (Fig. 3).
The modelling of press fit loading due to an interference of 0.28 mm related to the axle' diameter, comes from the use of gap elements (the corresponding normal gap value is equal to 0.14 mm) at the axle-hub interface (Fig. 3); moreover a frictional contact is considered with friction coefficient μ = 0.6. The latter kind of nonlinear loading involves an incremental-iterative solution procedure.

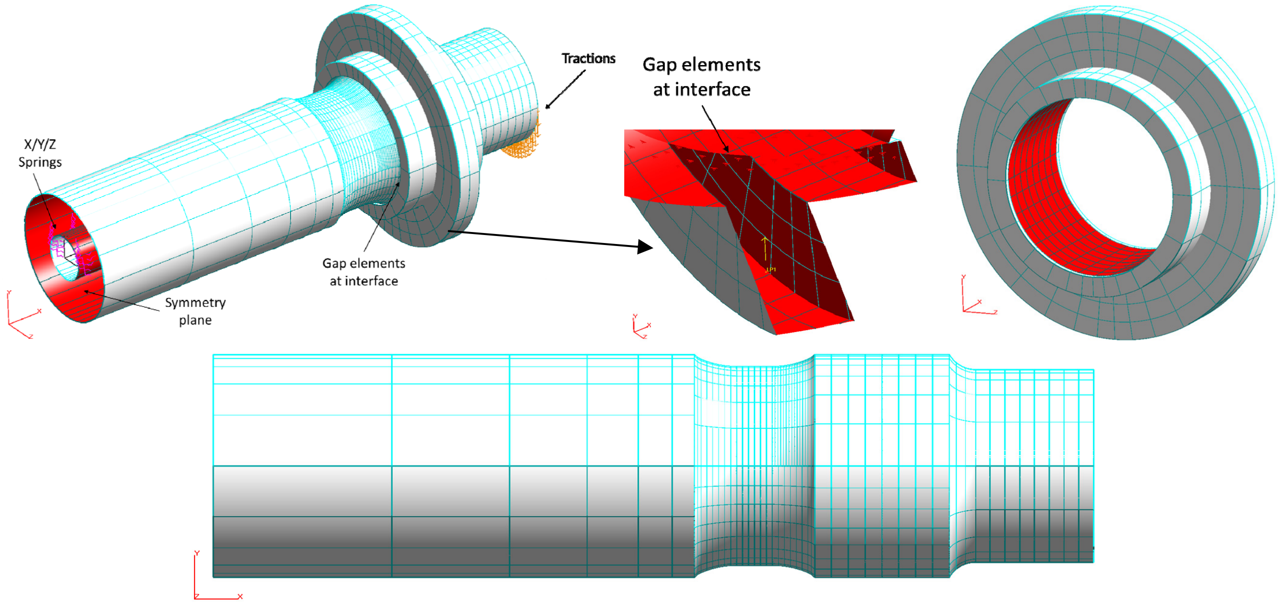

Figure 3: DBEM un-cracked model with highlight of mesh, yz symmetry plane, load introduction (tractions and point force) and modelling strategy, based on two distinct zones with normal gap (highlighted in red) at the axle-hub interface.

Cracked DBEM model

Subsequently to the DBEM stress analysis on the uncracked axle-hub coupling, a semi-elliptical crack has been inserted on the axle in the position shown in Fig. 4. After the crack insertion (that is fully automatic together with the inherent local remeshing), the number of quadratic elements and dofs increases from 2512 and 31650 to 3134 and 48621 respectively.

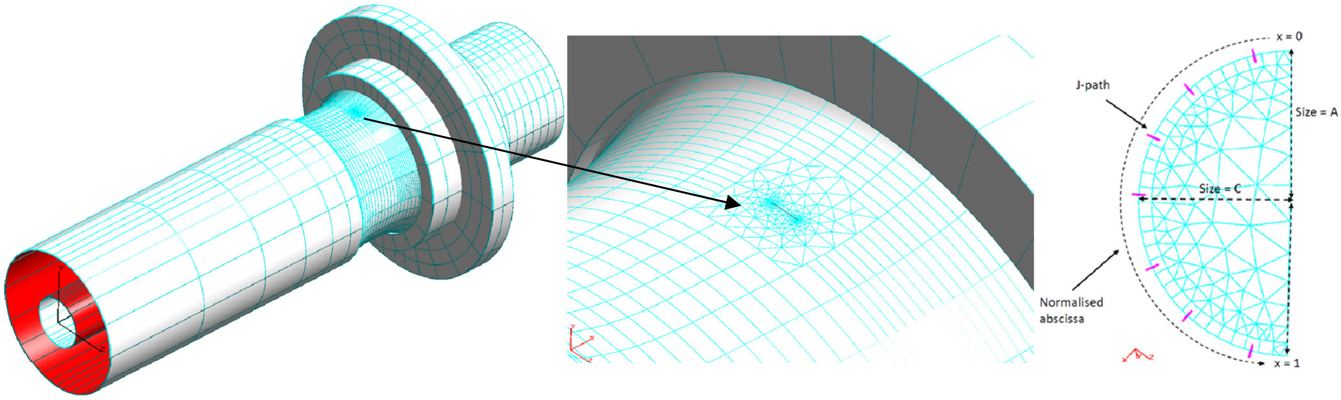

Figure 4: DBEM cracked model with close up of the re-meshed area surrounding the crack and details of the initial crack geometry (for the initial crack A=B=3.8 mm and C=1.9 mm).

DBEM (AND FEM) RESULTS

Uncracked DBEM model

For each of the three aforementioned load cases the Von Mises stress scenarios are presented (Figs. 5-7), in order to highlight the impact of each load case on the axle level of stress. The bending load case is responsible for high level of stresses in correspondence of the (red colored) area that will be selected for crack insertion (Fig. 5). Such area is clearly impacted by the press fit condition (Fig. 6) becoming a highly stressed area when the simultaneous application of both load cases is considered (red colored area to the left of hub insertion area in Fig. 7).

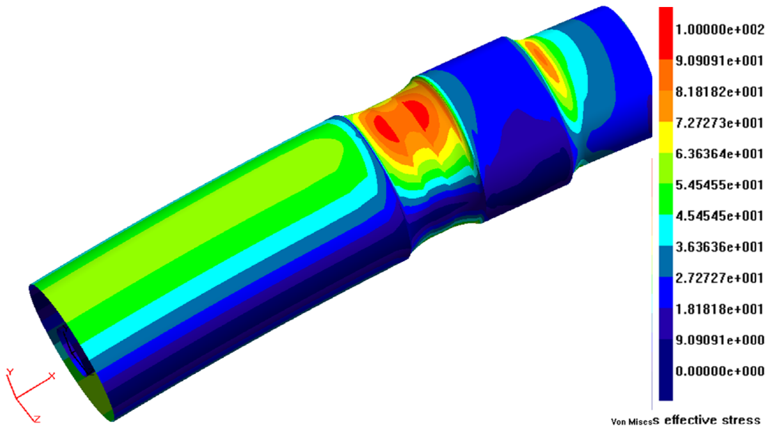

Figure 5: Deformed plot (scale factor 100) with Von Mises stresses [MPa] calculated for the bending load case.

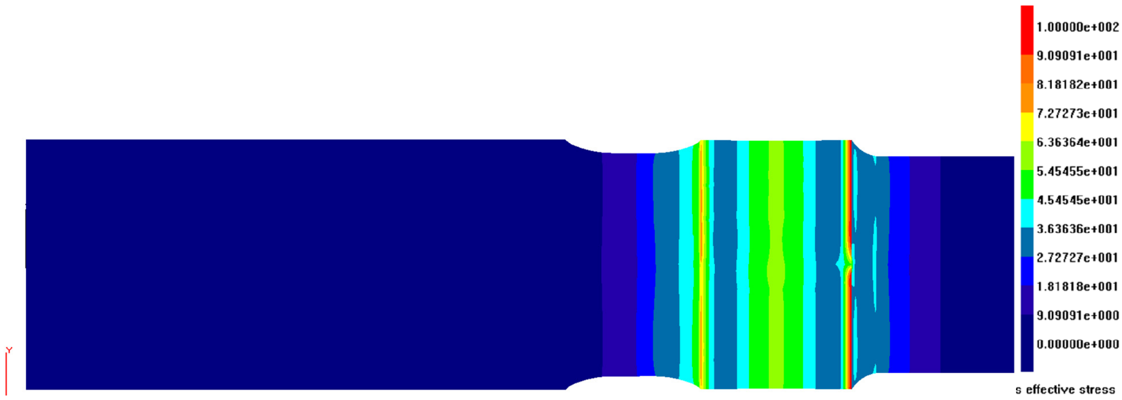

Figure 6: Deformed plot (scale factor 100) with Von Mises stresses [MPa] calculated for the press fit load case.

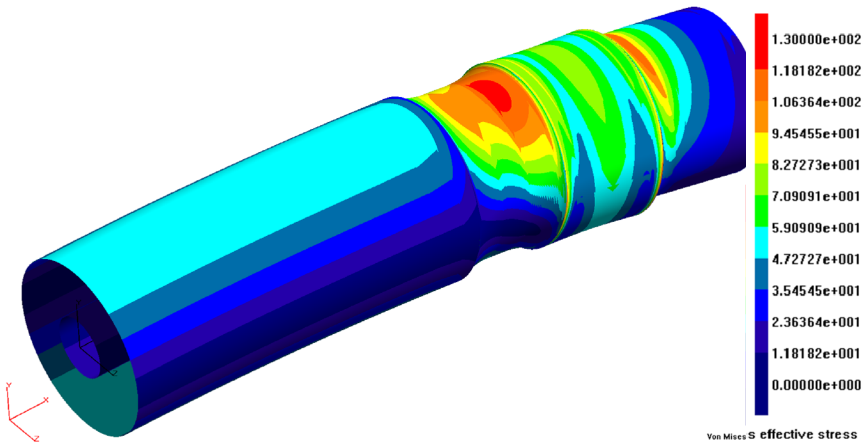

Figure 7: Deformed plot (scale factor 100) with Von Mises stresses [MPa] calculated for the coupled load case (press fit + bending).

Cracked DBEM model

From the previous analysis on the uncracked model the most critical area is pointed out and consequently the area of crack insertion can be effectively defined (Fig. 4). Again, the stress scenarios are calculated for the three aforementioned load cases (Figs. 8-10) and the SIF variation along the initial crack front for the combined bending+press fit load case is showed (Fig. 11a-c): a comparison is

displayed between SIFs calculated by DBEM when using COD or alternatively J-integral approaches; the comparison is extended to FEM (Finite Element Method) results obtained by the authors using the code ZENCRACK [15].
The DBEM results obtained by COD are less accurate as expected, because based on "standard" discontinuous elements along the crack front [2], with no use of quarter point elements as done in FEM crack modeling.

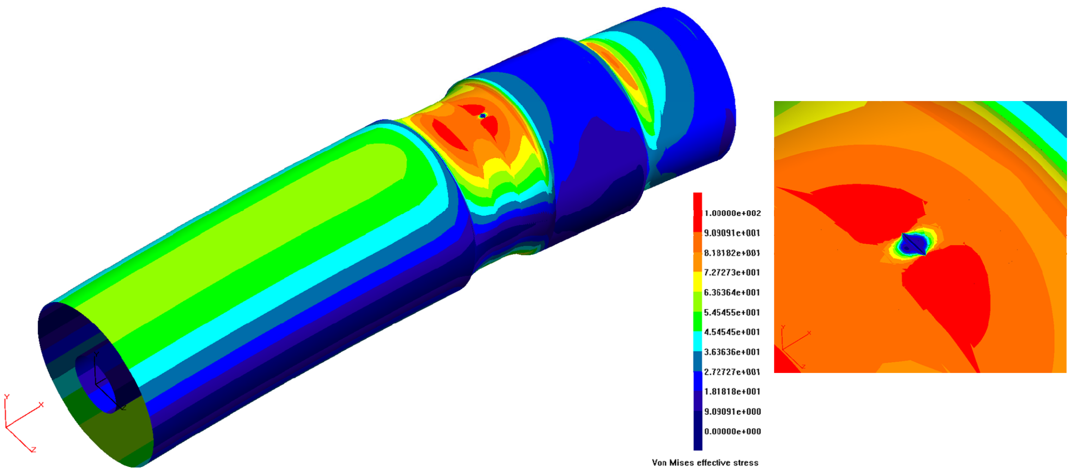

Figure 8: Deformed plot (scale factor 100) with Von Mises stresses [MPa] for the bending load case and close up of the cracked area.

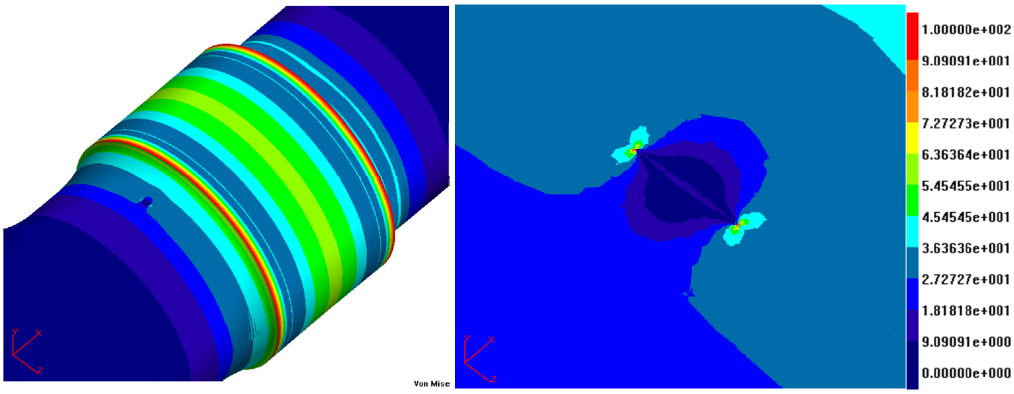

Figure 9: Deformed plot (scale factor 100) with Von Mises stresses [MPa] for the press fit cracked model and close up of the crack.

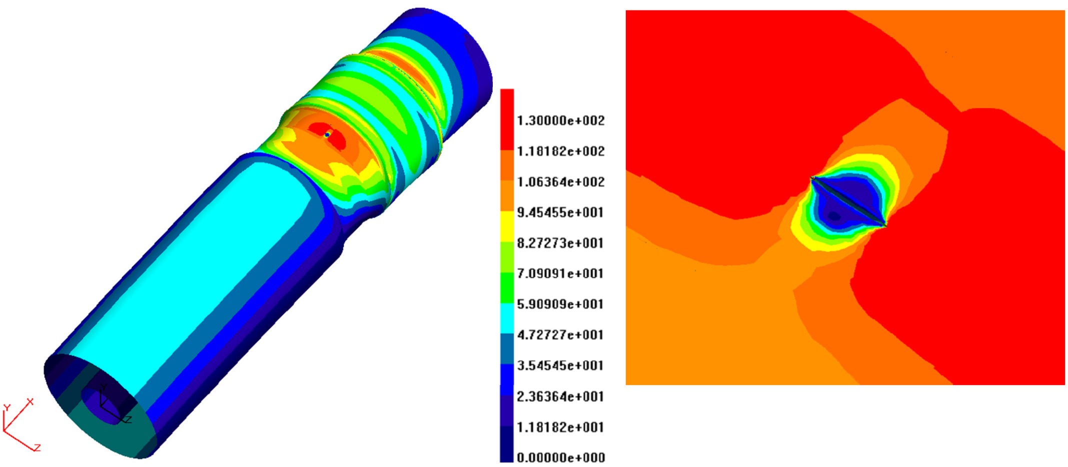

Figure 10: Deformed plot (scale factor 100) with Von Mises stresses [MPa] for the combined bending + press fit load case and close up of the cracked area.

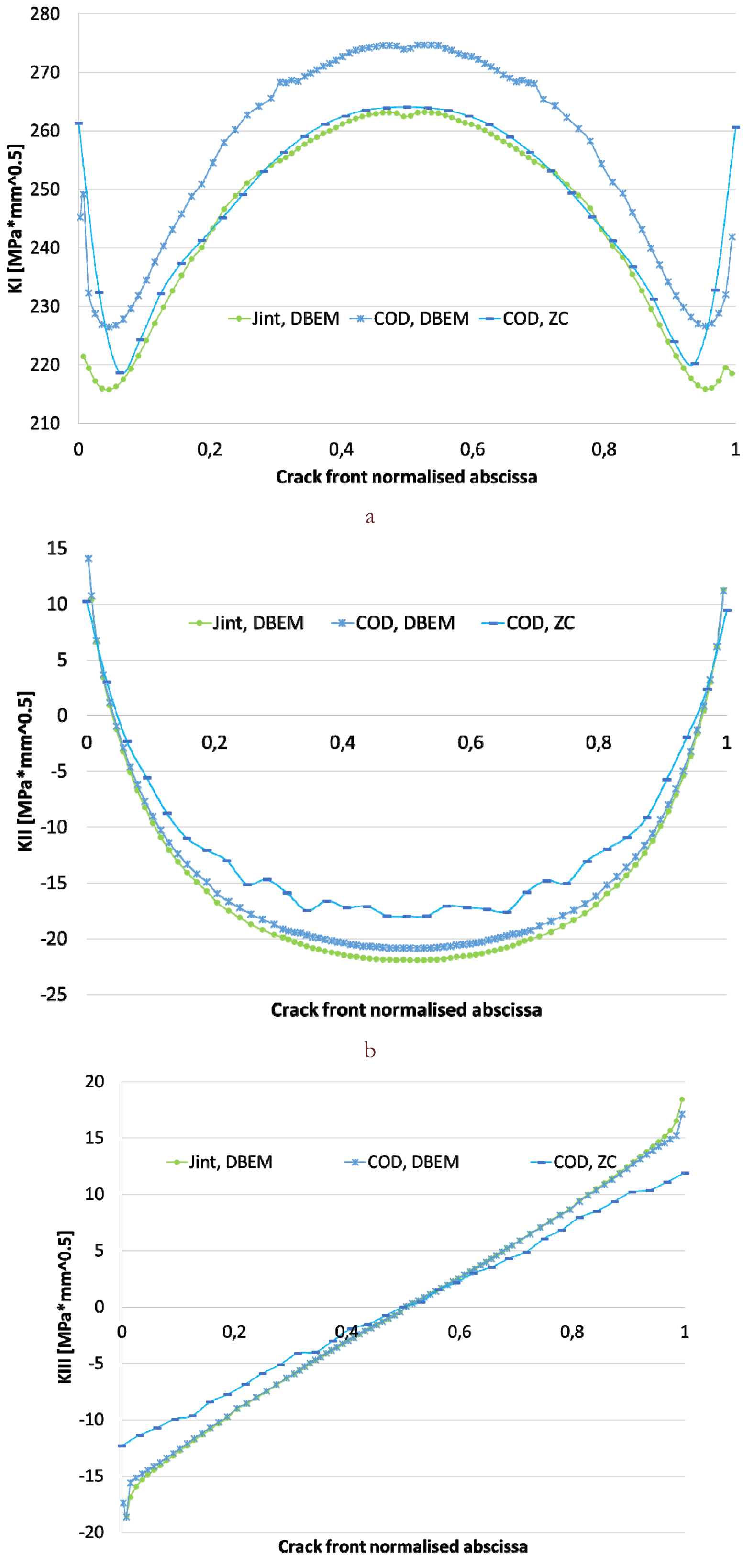

Figure 11a-c: SIF results along the initial crack front for the bending+press fit load case, calculated by COD and J-integral using the DBEM code BEASY and the FEM code ZENCRACK (ZC).

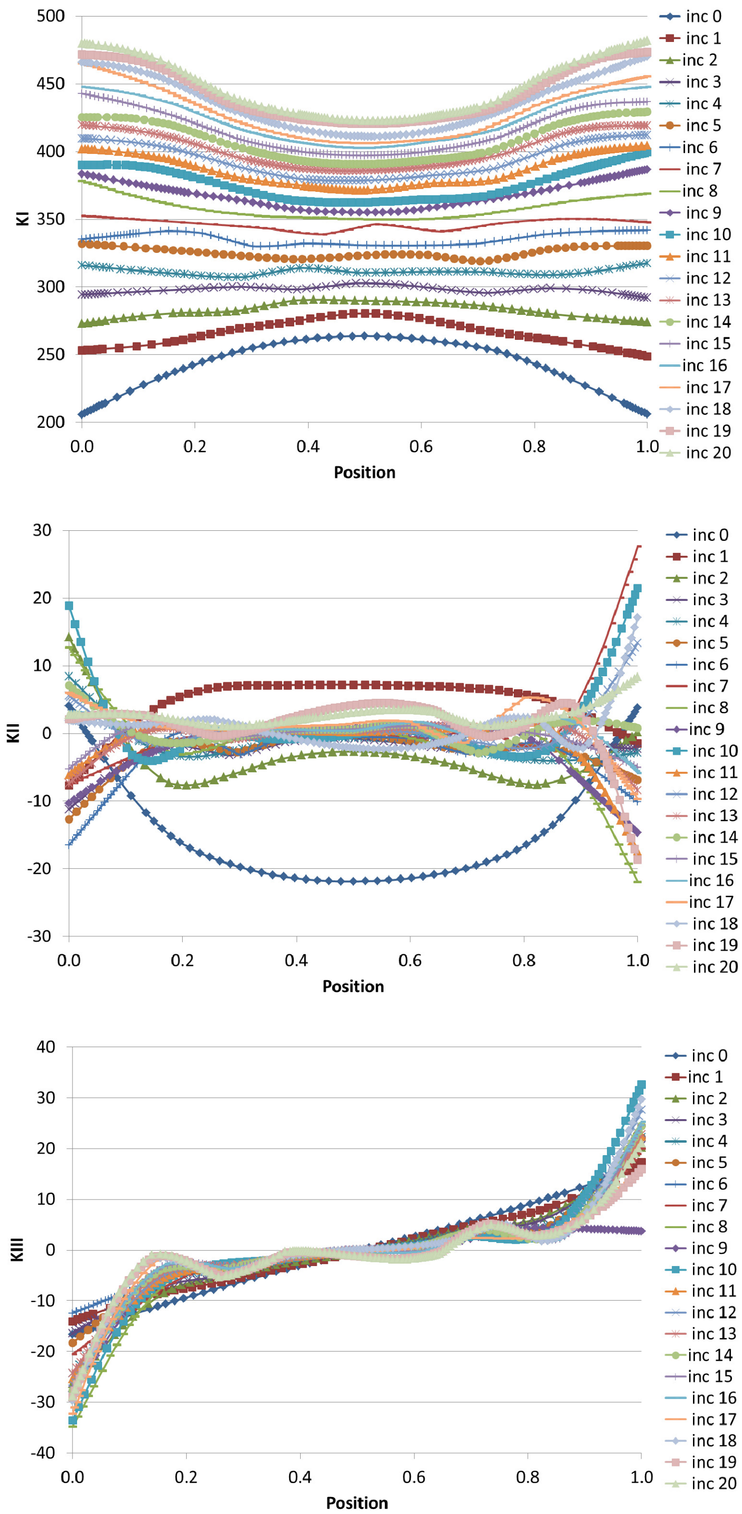

Figure 12: SIF results along selected crack fronts for the combined bending + press fit load case.

DBEM Crack propagation for the combined bending + press fit load case

The crack propagation simulation is splitted in 16 steps, with an average crack advance at each step equal to 0.5 mm, and with a fully automatic remeshing at each crack advance. SIFs along the crack fronts for the combined bending + press fit load case are plotted in Fig. 12: if initially there is a faster crack growth in the depth direction, after few steps the reverse happens with a faster crack advance at breakout points.

The crack growth rates are calculated with the NASGRO formula (Eq. 1) whose calibration parameters are reported in Tab. 1, whereas results in terms of crack sizes vs cycles are shown in Fig. 13. The crack shape variation during growth is shown in Fig. 14. Von Mises stresses on the final cracked scenario are showed in Fig. 15: it is possible to observe that as expected the propagation proceeds under nearly pure mode I with no appreciable crack kinking due to the prevailing bending load case.

$$\frac{da}{dN} = \frac{C \cdot \Delta K^n \cdot \left(1 - \frac{\Delta K_{th}}{\Delta K}\right)^p}{\left(1 - \frac{\Delta K}{(1-R) \cdot K_c}\right)^q} \tag{1}$$

Parameter	Value
C	1.23085 E-12
n	2.8
p	0.5
q	0.5
ΔK_{th}	152.89
K_c	5097.242

Table 1: NASGRO3 parameters (SIF units [MPa*mm$^{0.5}$] and growth rates units [mm/cycle]).

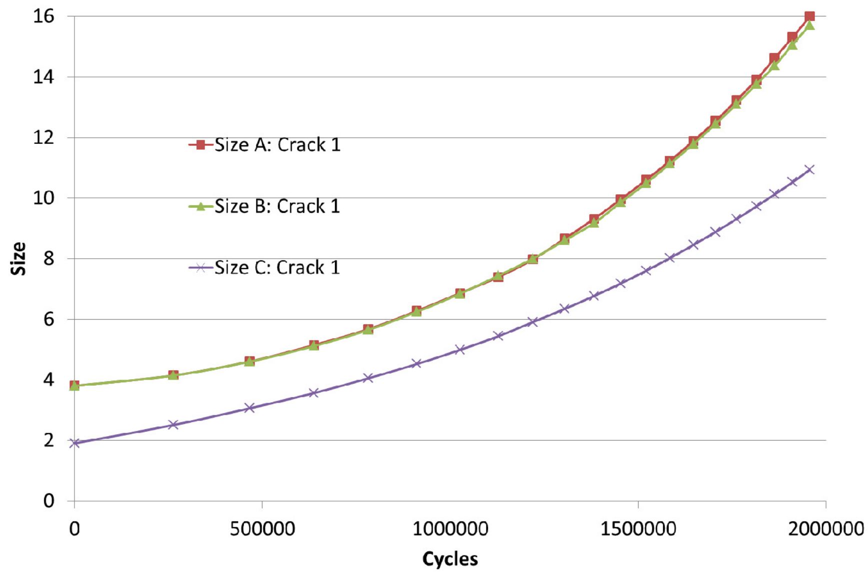

Figure 13: Crack sizes (mm) vs cycles: A and B are the crack length measured at break through points whereas C is the crack depth.

Conclusions

The impact on the crack behavior, and specifically on the SIF values along its front, of the superposition between the main bending loading case and the secondary axle-hub coupling interference is showed. A relevant impact of the press fit loading condition on the overall SIFs along the initial crack front is evident, suggesting the designer to accurately plan the level of interference values to be adopted when coupling hubs and axles.

There are some advantages when using DBEM rather than FEM for this kind of non-linear fracture problems: simplified modelling of the cracked area and accurate crack growth simulation especially when tackling contact loadings.

Further developments of this work will be devoted to resolution of the same problem by FEM in order to benchmark the two methodologies with reference to preprocessing effort, accuracy and runtimes, even if some results have already been anticipated in this paper showing a satisfactory level or correlation.

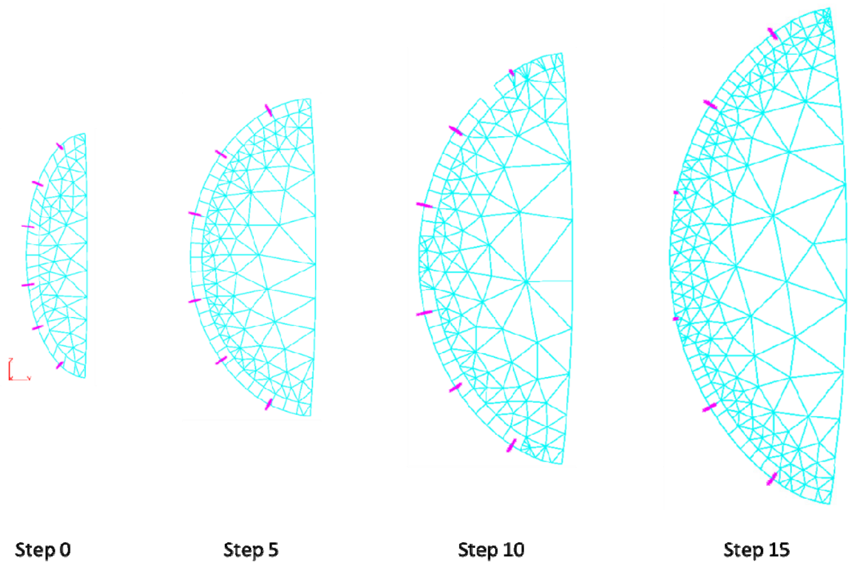

Figure 14: Crack shape during growth with highlight of J-paths along the crack front.

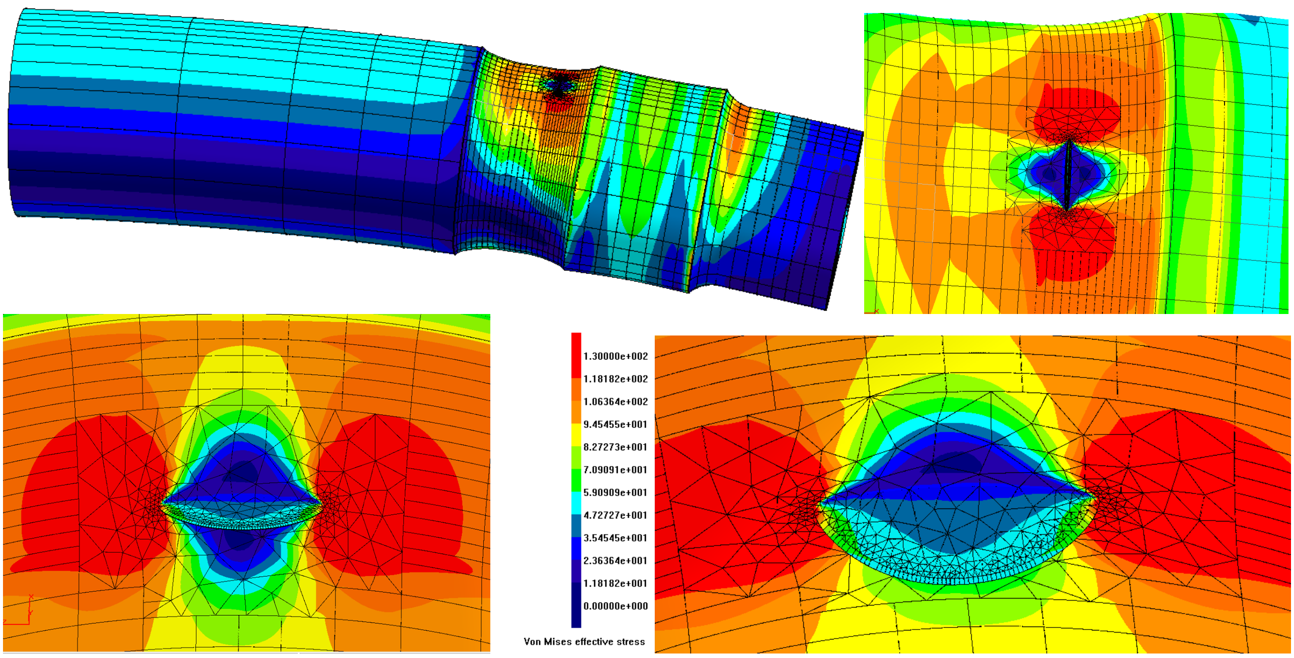

Figure 15: Deformed plot (scale factor 100) with Von Mises stresses [MPa] for the combined bending + press fit load case; close up of the cracked area with external (up) and internal views (down).

REFERENCES

[1] Portela A., In: Brebbia CA, Connor JJ, editors. Dual boundary element analysis of crack growth. Topics in engineering, vol. 14. Southampton: Computational Mechanics Publications, (1990).
[2] BEASY V10r14. Documentation. C.M. BEASY Ltd., (2011).
[3] Calì, C., Citarella, R., Perrella M., Three-dimensional crack growth: numerical evaluations and experimental tests, European Structural Integrity Society, Biaxial/Multiaxial Fatigue and Fracture, Edited by Andrea Carpinteri, Manuel de Freitas and Andrea Spagnoli, 31(3) (2003) 3-504.
[4] Citarella, R., Perrella, M., Multiple surface crack propagation: numerical simulations and experimental tests, Fatigue and Fracture of Engineering Material and Structures, 28 (2005) 135-148.
[5] Citarella, R., Soprano, A., Some SIF's evaluations by Dual BEM for 3D cracked plates, Journal of Achievements in Materials and Manufacturing Engineering, 19 (2) (2006) 64-72.
[6] Citarella, R., Buchholz, F.-G., Comparison of crack growth simulation by DBEM and FEM for SEN-specimens undergoing torsion or bending loading, Engineering Fracture Mechanics, 75 (2008) 489–509.
[7] Citarella, R., Cricrì, G., Lepore, M., Perrella, M., DBEM and FEM Analysis of an Extrusion Press Fatigue Failure. In: A. Öchsner, L.F.M. da Silva, H. Altenbach (eds.), Materials with Complex Behaviour–Advanced Structured Materials, 3(2) (2010) 181-191.
[8] Citarella, R., Cricrì, G., Comparison of DBEM and FEM Crack Path Predictions in a notched Axle under Torsion, Engineering Fracture Mechanics, 77 (2010) 1730-1749.
[9] Citarella, R., Lepore, M., Shlyannikov, V., Yarullin, R., Fatigue surface crack growth in cylindrical specimen under combined loading, Engineering Fracture Mechanics, 131 (2014) 439–453.
[10] Rigby, R.H., Aliabadi, M.H., Mixed-mode J-integral method for analysis of 3D fracture problems using BEM, Engng Anal Boundary Elem, 11 (1993) 239–56.
[11] Rigby, R.H., Aliabadi, M.H., Decomposition of the mixed-mode J-integral – revisited, Int J Solids Struct, 35(17) (1998) 2073–99.
[12] Citarella, R., Gerbino, S., BE analysis of shaft-hub couplings with polygonal profiles, Journal of Materials Processing Technology, 109 (2001) 30-37.
[13] Sih G.C., Strain energy density factor applied to mixed mode crack problems, Int J Fract, 10 (1974) 305-321.
[14] Lebahn, J., Sander, M., Benchmark zur numerischen Bestimmung von Spannungsintensitätsfaktoren in einer abgesetzten Welle. In: DVM-Bericht 245, Bruchmechanische Werkstoff- und Bauteilbewertung: Beanspruchungsanalyse, Prüfmethoden und Anwendungen, Deutscher Verband für Materialforschung und –prüfung e.V., Berlin, (2013) 147 – 156.
[15] ZENCRACK manual, Version 7.9.